Acta Astronautica 148 (2018) 186–204

Contents lists available at ScienceDirect

Acta Astronautica

journal homepage: www.elsevier.com/locate/actaastro

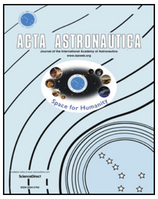

Failure tolerance strategy of space manipulator for large load carrying tasks

Gang Chen*, Bonan Yuan, Qingxuan Jia, Hanxu Sun, Wen Guo

School of Automation, Beijing University of Posts and Telecommunications, No 10 Xitucheng Rd., HaiDian-district, Beijing, 100876, China

ARTICLE INFO

Keywords:
Space manipulator
Failure tolerance
Large load carrying task
Task trajectory searching

ABSTRACT

During the execution of large load carrying tasks in long term service, there is a notable risk of space manipulator suffering from locked-joint failure, thus space manipulator should be with enough failure tolerance performance. A research on evaluating failure tolerance performance and re-planning feasible task trajectory for space manipulator performing large load carrying tasks is conducted in this paper. The effects of locked-joint failure on critical performance(reachability and load carrying capacity) of space manipulator are analyzed at first. According to the requirements of load carrying tasks, we further propose a new concept of failure tolerance workspace with load carrying capacity(FTWLCC) to evaluate failure tolerance performance, and improve the classic A* algorithm to search the feasible task trajectory. Through the normalized FTWLCC and the improved A* algorithm, the reachability and load carrying capacity of the degraded space manipulator are evaluated, and the reachable and capable trajectory can be obtained. The establishment of FTWLCC provides a novel idea that combines mathematical statistics with failure tolerance performance to illustrate the distribution of load carrying capacity in three-dimensional space, so multiple performance indices can be analyzed simultaneously and visually. And the full consideration of all possible failure situations and motion states makes FTWLCC and improved A* algorithm be universal and effective enough to be appropriate for random joint failure and variety of requirement of large load carrying tasks, so they can be extended to other types of manipulators.

1. Introduction

In space exploration, a large number of space tasks can hardly be completed relying only on human astronauts. As the typical on-orbit tool, space manipulator possesses the advantages of large span, flexible operation performance and powerful load carrying capacity, so it is no substitute for completing many on-orbit tasks [1,2], such as spacecraft transposition, space station assembly and maintenance, satellite recovery and release, and hovering aircraft auxiliary docking, etc. [3]. But for these tasks, the mass and inertia ratios of the load to manipulator itself can reach up to 20:1. And some large-scale space manipulators (Candarm2 for example) can carry the load whose mass and inertia are 70 times larger than manipulator itself [4]. These tasks are called large load carrying tasks, and they are precisely able to be completed by space manipulator because of the micro-gravity of space environment. For these tasks, space manipulator is required to be capable to track the desired trajectory with load on end-effector(EEF).

Generally speaking, space manipulator is designed to be qualified to the long term service in large load operation, but unavoidably, the output torque of joints usually stays at a high level, or even exceeds the nominal output of the driving motor sometimes. The proper functioning of a joint relies on coordinated operation of all components inside. However, in the case of carrying large load, many components are working in ultimate states. Taking an arbitrary joint for example, the driving motor, harmonic reducer and transmission device suffer from severe abrasion; the current in magnet exciting coil is very large and the motor goes through high temperature [5]; besides, its sensors may not collect accurate data, and it will further cause the disable feedback of control system. Therefore, the components of the joint are very likely to be broken, and the joint is prone to malfunction. Once joint failure occurs, space manipulator will lose original performance so that the task may fail [6]. Meanwhile, limited by the hazardous space environment, the fault joint can't be repaired or replaced immediately, so we wish the degraded space manipulator is still capable enough to complete the subsequent large load carrying task [7]. Thus, it is necessary to evaluate failure tolerance performance and re-plan task trajectory.

The fault joint is usually locked as long as any failure occurs to isolate failure, so it can't output motion and torque anymore [8]. But unfortunately, locked-joint failure will diminish the degrees of freedom (DOF) of space manipulator, and cause the degeneration of reachability [9], kinematics and dynamics dexterity [10,11], task execution ability [12] and load carrying capacity, and inevitably lead to the failure of subsequent tasks.

---

* Corresponding author. School of Automation, Beijing University of Posts and Telecommunications, No 10 Xitucheng Rd., Haidian-district, Beijing, 100876, China.
E-mail addresses: buptcg@163.com (G. Chen), yuanbonan@126.com (B. Yuan), spacerobot@163.com (Q. Jia), srobot@126.com (H. Sun), gw_0426@bupt.edu.cn (W. Guo).

https://doi.org/10.1016/j.actaastro.2018.04.052
Received 26 July 2017; Received in revised form 26 March 2018; Accepted 29 April 2018

Nomenclature

$\boldsymbol{a}_{k-1}$	The vector from the k^{th} joint to the centroid of the k^{th} link in the coordinate frame of the k^{th} joint
$\boldsymbol{b}_{k-1}$	The vector from the centroid of the k^{th} link to the $(k+1)^{\text{th}}$ joint in the coordinate frame of the k^{th} joint
C_{k-1}	The centroid of the k^{th} link
${}^{I}\boldsymbol{f}_{k}$	The force that the $(k+1)^{\text{th}}$ link exerts on the k^{th} link in inertia frame
${}^{I}\boldsymbol{f}_{e}$	Operating force exerting on the end-effector in inertia frame
${}^{I}\boldsymbol{F}_{k}$	Inertia force applied to the centroid of the k^{th} link in inertia frame
$\boldsymbol{I}_{k-1}$	The centroid of the k^{th} link in the coordinate frame of the k^{th} joint
J_{k-1}	The centroid of the k^{th} link
$\boldsymbol{l}_{k-1}$	The vector from the k^{th} joint to the $(k+1)^{\text{th}}$ joint in the coordinate frame of the k^{th} joint
m_{k-1}	Mass of the k^{th} link
${}^{I}\boldsymbol{n}_{k}$	The moment that the $(k+1)^{\text{th}}$ link exerts on the k^{th} link in inertia frame
${}^{I}\boldsymbol{n}_{e}$	Operating moment exerting on the end-effector in inertia frame
${}^{I}\boldsymbol{N}_{k}$	Inertia moment applied to the centroid of the k^{th} link in inertia frame
${}^{I}\boldsymbol{p}_{k-1}$	Position vector of the k^{th} joint in inertia frame
$\boldsymbol{q}$	Angular displacement vector of the joint, where $\boldsymbol{q} = [q_1, q_2, \cdots, q_n]^{\mathrm{T}} \in \mathbf{R}^{n\times 1}$
$\dot{\boldsymbol{q}}$	Angular speed vector of the joint, where $\dot{\boldsymbol{q}} = [\dot{q}_1, \dot{q}_2, \cdots, \dot{q}_n]^{\mathrm{T}} \in \mathbf{R}^{n\times 1}$
$\ddot{\boldsymbol{q}}$	Angular acceleration vector of the joint, where $\ddot{\boldsymbol{q}} = [\ddot{q}_1, \ddot{q}_2, \cdots, \ddot{q}_n]^{\mathrm{T}} \in \mathbf{R}^{n\times 1}$
${}^{I}\boldsymbol{r}_{e}$	Position vector of the end-effector in inertia frame
${}^{I}\boldsymbol{r}_{B}$	Position vector of the centroid of spacecraft base in inertia frame
${}^{I}\boldsymbol{r}_{k-1}$	Position vector for the centroid of the k^{th} link in inertia frame
${}^{I}\boldsymbol{R}_{k-1}$	Attitude matrix from k^{th} joint's frame to inertia frame
${}^{k-1}\boldsymbol{R}_{k}$	Attitude matrix from the $(k+1)^{\text{th}}$ joint's frame to the k^{th} one
${}^{I}\boldsymbol{v}_{k}$	Centroid speed of the k^{th} link in inertia frame
${}^{I}\dot{\boldsymbol{v}}_{k}$	Centroid acceleration of the k^{th} in inertia frame
$\boldsymbol{X}$	Position-orientation vector of the end-effector in inertia frame
$\dot{\boldsymbol{X}}$	Velocity of the end-effector in inertia frame
$\ddot{\boldsymbol{X}}$	Acceleration of the end-effector in inertia frame
${}^{I}\boldsymbol{z}_{k-1}$	Unit vector of the k^{th} joint's axis direction in inertia frame
${}^{I}\omega_{k}$	Angular velocity of the k^{th} link in inertia frame
${}^{I}\dot{\omega}_{k}$	Angular acceleration of the k^{th} link
$\boldsymbol{\tau}$	Torque vector of joint, where $\boldsymbol{\tau} = [\tau_1, \tau_2, \cdots, \tau_n]^{\mathrm{T}} \in \mathbf{R}^{n\times 1}$
$\sum_{I}$	Inertial coordinate frame
$\sum_{B}$	Coordinate frame of manipulator's base
$\sum_{n}$	Coordinate frame of end-effector
$\sum_{k-1}$	Coordinate frame of the k^{th} link

In order to complete a large load carrying task, space manipulator is basically required to track the reachable trajectory with enough load carrying capacity, so the failure tolerance performance evaluation of reachability and load carrying capacity should be carried out. Presently, the evaluation methods of reachability have been extensively studied, but there are few researches on failure tolerance load carrying capacity. Moreover, the researches on failure tolerance reachability evaluation mostly aim at the low-DOF manipulator, and the existing evaluation methods are too complex to be applied to the space high-DOF manipulator. In order to take the degraded space manipulator into failure tolerance load carrying task as soon as possible, a comprehensive failure tolerance performance evaluation approach, which can evaluate failure tolerance reachability and load carrying capacity simultaneously, is proposed in this paper.

Many researchers evaluated the reachability after joint failure with failure tolerance workspace(FTW), and FTW can illustrate the reachable range visually. Due to the movement limitation of fault joint, FTW degrades compared to the normal workspace [13]. The solving approaches of FTW mainly include analytic method [14], geometric method [15] and numerical method [15]. The normal workspace and FTW of 3-DOF manipulator were established by Zhou [16] and Paredis [15] based on analytic method and geometric method respectively. Combining the analytic and the geometric method, the accurate boundary of FTW for plane manipulator was calculated by Hoover [17]. Researches above demonstrate that the accurate boundary of FTW can be determined by analytic and geometric methods, but when it comes to high-DOF manipulator, these methods are too complicated.

By contrast, the approximate shape and boundary of the workspace can be determined effectively by numerical method, so it can be used for qualitative analysis and geometric verification of FTW. Considering the dynamics coupling of 3-DOF space manipulator, a numerical method for the workspace in fixed base state, free-flying state and free-floating state was deduced by Xu [18], but in order to avoid dynamics singularity, too many factors should be considered. Chen [19] briefly described Monte Carlo method in numerical method, and gave the main solving process for FTW of high-DOF manipulator. However, he mainly concentrated on the solving of workspace boundary, and the specific application of the Monte Carlo method was not given enough attention. The analysis of FTW can be achieved by various methods, but for the sake of quick recovery of space manipulator in post-failure tasks, the fast evaluation for the reachability is significant. Generally speaking, space manipulator possesses complex structure, and the shape of its workspace is always irregular, so we focus on the simulation statistical idea in Monte Carlo method, and traverse in operational range of the rest healthy joints to generate FTW quickly. In FTW, the reachable task trajectory that connects the initial and the desire point can be found out.

Besides the reachable task trajectory, enough load carrying capacity is also a fundamental requirement to finish post-failure load carrying task. Load carrying capacity is defined as the maximum payload that the manipulator can repeatedly lift, and its value is affected by many factors, such as deformation constraints of flexible links and joints, nominal output of joints. For the flexible ground manipulator, effect of the flexural deformation of links on load carrying capacity was pointed out by Ding [20]. Aiming at the ground 9-DOF manipulator, Shan [21] studied load carrying capacity on the basis of strength, stiffness and modal analysis to links. Optimizing the structure parameters of manipulator with redundant joints, the load carrying capacity was improved by Zhang [22]. Researches above analyze the limitations of load carrying capacity that come from manipulator structure parameters, but apart from factors above, load carrying capacity of space manipulator is mainly limited by base disturbance [23] and maximum output of joints [24]. Some constraints about base pose perturbation and joint kinematics parameters were proposed by Korayem [25–27], and furthermore, the change rule of load carrying capacity was described. Considering the limitation of joint torque and base perturbation, Jia [28] designed a trajectory optimization strategy for space manipulator through maximizing the load carrying capacity. Moreover, the paper proved that joint torque and base pose perturbation were determined by motion states, so load carrying capacity was further affected. In consequence, the load carrying capacity mainly depends on the self-constraints of manipulator and current motion states.